Signature splitting and magnetic rotation in ^{86}Y

Jian Li (李剑),[1,*] C. Y. He (贺创业),[2,†] Y. Zheng (郑云),[2] C. B. Li (李聪博),[2] K. Y. Ma (马克岩),[1] and J. B. Lu (陆景彬)[1,‡]

[1]*College of Physics, Jilin University, Changchun 130012, China*

[2]*China Institute of Atomic Energy, Beijing 102413, China*

(Received 13 March 2013; revised manuscript received 22 May 2013; published 19 July 2013)

Based on recent experimental data, the band structure of the odd-odd nucleus ^{86}Y has been studied. The positive-parity yrast band built on the configuration $\pi g_{9/2} \otimes \nu g_{9/2}^{-1}$ shows a large signature splitting, and a signature inversion occurs at $I \sim 13\hbar$. The signature inversion is interpreted by the competition between single-particle and collective excitations in this nucleus. The negative-parity dipole band, which is probably connected with magnetic rotation, is assigned to the configurations $\pi g_{9/2}^2(p_{3/2}/f_{5/2})^{-1} \otimes \nu g_{9/2}^{-1}$ before and to $\pi g_{9/2}^2(p_{3/2}/f_{5/2})^{-1} \otimes \nu g_{9/2}^{-3}$ after the alignment. Self-consistent titled axis cranking calculations based on relativistic mean-field theory are performed to interpret the rotational structure. Characteristic features of magnetic rotation are found for the negative-parity band.

DOI: 10.1103/PhysRevC.88.014317 PACS number(s): 21.10.Re, 21.60.Jz, 23.20.Lv, 27.50.+e

I. INTRODUCTION

Nuclei in the f-p-g shell are very sensitive to polarization effects of individual particles on the high-j orbital. The shapes strongly depend on the number of protons Z and neutrons N, on rotation, and on the orbitals occupied by the quasiparticles. With increasing neutron number towards the neutron shell closure at $N = 50$, the deformation-driving features diminish. For the nuclei in between, an enhanced transitional character leads to a very fragile coexistence of excitation modes based on different deformations. Especially in the nuclei with 47 neutrons, the intruder subshell $g_{9/2}$ is more than half filled and has lost most of its deformation driving capability [1,2]. Therefore, they provide an excellent laboratory for studying the interplay between single-particle and collective excitations. In ^{84}Rb [2], signature inversion occurs in its positive-parity band with rotation-like structures. Comparing different isotopes of this nucleus, the inversion point is shifted slightly to higher spins with increasing neutron number. For the nuclei with two more protons, the high-spin structure of ^{80,82,84}Y [3–5] has been well studied and signature inversion has also been observed in their positive-parity bands. The investigation of ^{86}Y is motivated by the question of how this structural evolution is developing for the Y isotopes with increasing neutron number.

In addition, magnetic rotation (MR) [6,7], which has been successfully described by the titled axis cranking (TAC) model and which has been extensively studied in the mass regions $A \sim 110$ [8–10], $A \sim 130$ [11,12], and $A \sim 200$ [13,14], is also an interesting phenomenon in the $A \sim 80$ mass region. For instance, as the deformation-driving features diminish with increasing neutron number towards the neutron shell closure at $N = 50$, magnetic rotational bands with negative parity were observed in ^{82,84}Rb [15–17]. In a systematic study, it is probably possible to find similar rotational modes in the neighboring isotones, such as ^{86}Y.

Recently, high-spin states in ^{86}Y have been studied by Rusu *et al.* [18] using heavy-ion fusion-evaporation reactions. The yrast sequence has been extended and $M1$ bands with negative parity have been observed in ^{86}Y. The corresponding level structures were interpreted by shell-model calculations. These authors also emphasize the need for theoretical investigations of a possible magnetic rotation with negative parity, in particular within the tilted axis cranking approximation [19].

In this paper, we shall first present discussions of the signature inversion in the positive-parity band, and then use the recently established self-consistent relativistic tilted axis cranking theory (TAC-RMF) [20–22] to investigate the dipole structures in ^{86}Y as candidates for magnetic rotation.

II. SIGNATURE SPLITTING IN THE POSITIVE-PARITY BAND

In Fig. 1, we replot the level scheme of the yrast band and the newly established negative-parity band in ^{86}Y obtained from Ref. [18]. The yrast band of the odd-odd nucleus ^{86}Y is built on the $8^{(+)}$ isomeric state located at 218 keV above the 4^- ground state. This band has been extended in Ref. [18] up to a $17^{(+)}$ state with an energy of 5993 keV. Its configuration has been already assigned in Ref. [23] to $\pi g_{9/2} \otimes \nu g_{9/2}^{-1}$. This has been also confirmed by shell-model calculation in Ref. [18]. In general, many similarities can be found between rotational bands in nearby nuclei if they are built on the same intrinsic quasiparticle (qp) structure. This is the case for the positive-parity yrast bands of odd-odd nuclei in the $A \sim 80$ mass region, which are well described theoretically by the occupation of two unlike $g_{9/2}$ nucleons [24–26]. The rotational hypothesis can be tested by comparing the kinematic moments of inertia $J^{(1)}$ [27,28] with those of the yrast bands of nearby odd-odd nuclei. These quantities, deduced from experimental energies and spins, are often used as a measure of the change of collectivity between nuclear rotational bands.

*jianli@jlu.edu.cn
†chuangye.he@gmail.com
‡ljb@jlu.edu.cn

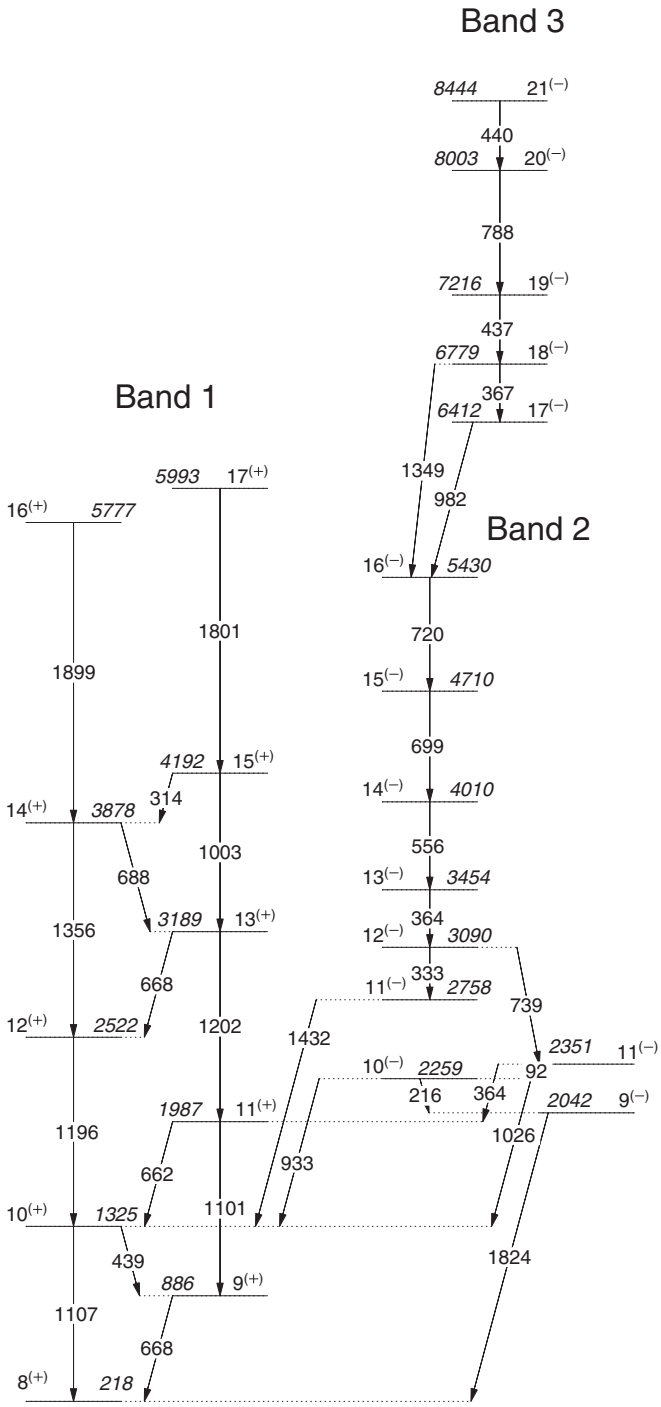

FIG. 1. Level scheme of positive-parity and negative-parity bands in ^{86}Y obtained from Ref. [18]. The energies of the γ transitions and of the levels are given in keV. Parentheses denote that the parities are assigned tentatively.

In Fig. 2 we show the kinematic moments of inertia $J^{(1)}$ for the positive-parity band in ^{86}Y. For comparison we also present the values for the corresponding bands in ^{84}Rb [2] and ^{84}Y [5]. It can be seen that for ^{86}Y the $J^{(1)}$ value is about 18 $\hbar^2$MeV^{-1} at $I = 9\hbar$, and it remains (except for $I = 14\hbar$) for higher angular momenta nearly constant, ranging from 18 to 20 $\hbar^2$MeV^{-1}, which is close to the rigid-body value of nuclei in the

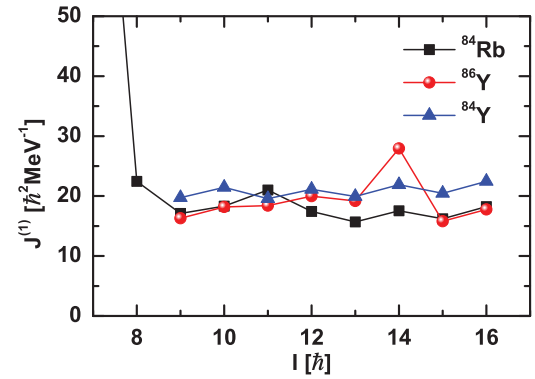

FIG. 2. (Color online) Kinematic moments of inertia $J^{(1)}$ as a function of spin for the positive-parity yrast bands in ^{86}Y, ^{84}Rb, and ^{84}Y.

$A \sim 80$ mass region [16,25]. As shown in Fig. 2 this behavior is rather similar to that in the nearby odd-odd nuclei ^{84}Rb and ^{84}Y. The relatively constant values of $J^{(1)}$ in a relatively large range of spins suggest a collective rotation for high-spin states in the yrast band. However, before a lifetime measurement, further theoretical investigations about the collectivity could include the study of nuclear deformation in self-consistent relativistic mean field calculations [29] and the comparison of the rotational structure with that deduced from the particle rotor model [30].

One attractive feature of almost all odd-odd nuclei in this region is the large signature splitting in the positive-parity yrast band and a reversal of the splitting pattern near spin $I = 9\hbar$. It has been pointed out earlier [24] that the signature inversion in the $A \sim 80$ mass region is related to the filling of the high-j $g_{9/2}$ proton and $g_{9/2}$ neutron subshells, and that reflects the transition from mainly single-particle excitations at low spins to more rotational, i.e., collective, motion at higher spins. It can be well visualized by plotting the experimental quantity $[E(I) - E(I-1)]/2I$ as a function of spin. This is shown in Fig. 3 for the yrast bands of ^{86}Y, ^{84}Rb [2], and ^{84}Y [5].

The pattern for each graph shown in Fig. 3 is essentially the same. At higher spins, beyond the level crossing, the odd-spin states (filled circles) are increasingly low in energy and display a relatively high degree of signature splitting. This agrees with the theoretical expectation that odd-spin states should be favored for rotational bands built on the $\pi g_{9/2} \otimes \nu g_{9/2}^{-1}$ configuration. At low spins, the even-spin states (opened circles) are lower in energy and the degree of signature splitting is reduced. The splitting pattern is one of the indicators for nuclear collectivity. A reduced splitting may indicate that rotation plays a less important role at low spins than at high spins. Near the region of $I^\pi = 13^{(+)}\hbar$, there is an inversion in the phase of the pattern for ^{86}Y. In the other two cases ^{84}Rb [2] and ^{84}Y [5], the inversion point occurs at about $I^\pi = 11^{(+)}\hbar$.

A rather similar signature inversion was predicted near $I = 9\hbar$ in ^{76}Br and ^{82}Y on the basis of two-qp-plus-rotor calculations [24,25]. In these calculations, the change in signature splitting represents the onset of collective rotation above the maximum spin available for two unlike $g_{9/2}$ qp's, namely, $9\hbar$. At low spins the increase in spin comes mainly from recoupling of the two qp's, while collective rotation dominates above the

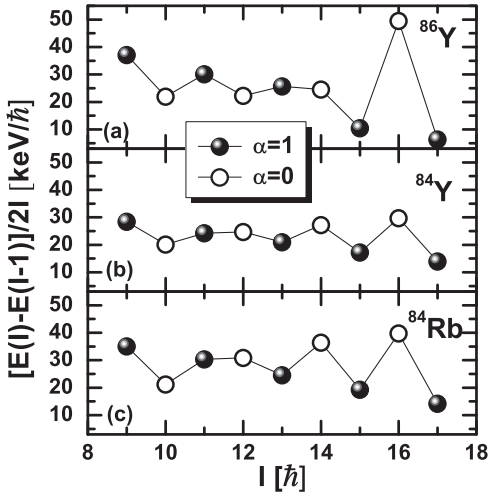

FIG. 3. Plot of the quantity $[E(I) - E(I-1)]/2I$ as a function of spin for the positive-parity yrast bands in ^{86}Y, ^{84}Y [5], and ^{84}Rb [2]. Solid (open) circles represent signature $\alpha = 1$ even-spin sequence ($\alpha = 0$ odd-spin sequence).

reversal point. With increasing proton or neutron number, the small shift of the inversion point to higher spins is also likely due to the competition between single-particle and collective degrees of freedom. With nucleon numbers increasing up to the shell closure $N = 50$, single-particle character plays a more and more important role at lower spin states, and remains important to slightly higher spins for excited states. This could be a possible reason for the rise of the inversion point.

III. MAGNETIC ROTATION IN THE NEGATIVE-PARITY BAND

As shown in Fig. 1, the negative-parity band built on the $I = 11\hbar$ state located at 2758 keV above the 4^- ground state [31] is mainly composed of a series of dipole transitions, and has been extended in Ref. [18] up to the $I^\pi = 21^{(-)}$ state with the energy 8444 keV. The large energy separation to the ground state and other low-lying states indicates a predominantly four-quasiparticle nature in the negative-parity band. The decay out at the $I^\pi = 11^{(-)}$ bandhead state happens only to the $I^\pi = 10^{(+)}$ state of the yrast band, and it further supports a four-quasiparticles nature of the bandhead. In ^{86}Y, the proton Fermi level is located near the Nilsson orbitals $2p_{3/2}$, $2p_{1/2}$, $1f_{5/2}$ and the high-j orbital of the $\pi g_{9/2}$ subshell, while the neutron Fermi level lies at the upper end of the $\nu g_{9/2}$ subshell. Thus the proton or neutron configurations may include the filling of these orbitals. In fact, it has been pointed out in Refs. [15,16] that the lowest-lying four-quasiparticle (4qp) configuration for the neighboring nuclei with $Z = 37$ and $N = 45, 47$ turns out to be $\pi g_{9/2}^2(p_{3/2}/f_{5/2})^{-1} \otimes \nu g_{9/2}^{-1}$.

To investigate its structure, the experimental angular momentum is shown in Fig. 4 as a function of rotational frequency for the negative-parity band in ^{86}Y. The experimental rotational frequency has been extracted as in Ref. [32],

$$\hbar\omega = \frac{1}{2}[E_\gamma(I+1 \to I) + E_\gamma(I \to I-1)] \approx \frac{dE}{dI}. \qquad (1)$$

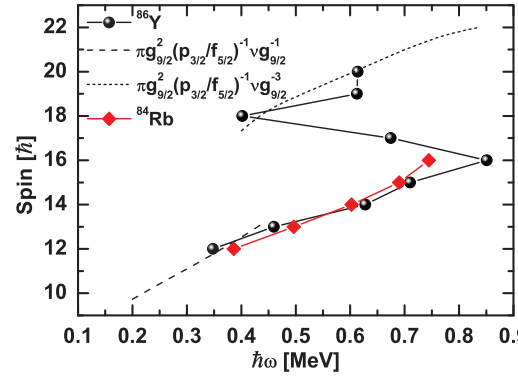

FIG. 4. (Color online) Angular momentum as a function of rotational frequency for the negative-parity band in ^{86}Y, in comparison with TAC-RMF calculations and similar $M1$ bands in ^{84}Rb.

It is easy to see that in the negative-parity band of ^{86}Y a backbend is observed at spin $17\hbar$.

In contrast with its isotone ^{84}Rb [2], a similar $M1$ band has also been observed in its level structure, and it has been interpreted as magnetic rotation band based on the $\pi g_{9/2}^2(p_{3/2}/f_{5/2})^{-1} \otimes \nu g_{9/2}^{-1}$ configuration [15,17]. For comparison we show in Fig. 4 the observed spins I as functions of the rotational frequency ω for the similar band in ^{84}Rb [15,17]. It is clear that both nuclei show almost the same behavior, and the striking similarities in excitation energy have been shown already in Ref. [18]. Therefore, before the backbend of the negative-parity band, ^{86}Y may have the same configuration as the $M1$ band in ^{84}Rb.

For the higher spin states of the negative band in ^{86}Y, the backbend shown in Fig. 4 is possibly attributed to the alignment of a neutron pair in the $g_{9/2}$ orbital with a gain in angular momentum. It also has been proposed by shell-model calculations in Ref. [18] that the high-spin states have the largest components characterized by the coupling of three neutron holes in the $g_{9/2}$ orbital with one proton hole and a broken pair of protons in the $f_{5/2}$ and $g_{9/2}$ orbitals, respectively. Thus, after backbend in the negative band, the corresponding configuration could be $\pi g_{9/2}^2(p_{3/2}/f_{5/2})^{-1} \otimes \nu g_{9/2}^{-3}$. Moreover, the shell-model calculation in Ref. [18] predicts strong $M1$ transitions in the negative band. All of the indications show that the negative-parity band may have the nature of a shears mechanism, and is thought of tentatively as a MR band. In the following, we perform the TAC-RMF calculations [21] to study the candidate for the MR band.

TAC-RMF theory is based on sophisticated covariant density functional theory (CDFT). During the past two decades, CDFT has received wide international attention due to its success in describing many nuclear phenomena in stable as well as in exotic nuclei [33–35]. On the basis of the same functional and without any additional parameters, the rotational excitations can be described in practical applications within the TAC-RMF framework. In Ref. [36], cranked RMF theory with arbitrary orientation of the rotational axis, i.e., three-dimensional cranking, has been developed. However, due to its numerical complexity, it has only been applied for the magnetic rotation in ^{84}Rb [36]. Focusing on magnetic rotation, the cranked RMF model was improved greatly

and a two-dimensional cranking version of the RMF model based on a nonlinear meson-exchange interaction has been established [20]. Very recently, the TAC model based on relativistic point-coupling Lagrangians was constructed with further simplifications [21]. This version is more suitable for systemic investigations. This self-consistent TAC-RMF model based on a point-coupling interaction has been applied to shears bands in the nuclei ^{58}Fe [37], ^{60}Ni [21], ^{113,114}In [10,38], and ^{198,199}Pb [39]. Furthermore, with the same density functional PC-PK1 [40] antimagnetic rotational bands were also successfully described in the nuclei ^{105}Cd [41,42] and ^{112}In [43]. For a review of TAC-RMF theory and its application in nuclear magnetic rotation, see Ref. [22].

For the present calculations, self-consistent two-dimensional cranked RMF theory [21] is used for the parameter set PC-PK1 [40] in order to examine the shears mechanism in the nucleus ^{86}Y, while pairing correlations are neglected. The Dirac equation for the nucleons is solved in a three-dimensional harmonic oscillator basis [44], and a basis of eight major oscillator shells is adopted. For the nucleus ^{86}Y, the negative-parity $M1$ band has been calculated based on the configurations $\pi g_{9/2}^2(p_{3/2}/f_{5/2})^{-1} \otimes \nu g_{9/2}^{-1}$ before the alignment and $\pi g_{9/2}^2(p_{3/2}/f_{5/2})^{-1} \otimes \nu g_{9/2}^{-3}$ after the alignment.

The calculated total angular momenta are also given in Fig. 4 as functions of the rotational frequency for the negative-parity band and are compared with the experimental data. It is found that the calculated results agree well with the experimental data both before and after the backbend, which further supports the configuration assignment. This also indicates that the present TAC-RMF calculations can reproduce the relative changes of the moment of inertia within the different bands rather well. In addition, the TAC calculations also support that the backbend arises through an excitation of a neutron-hole pair in the $g_{9/2}$ shell, i.e., by the transitions in the configurations $\pi g_{9/2}^2(p_{3/2}/f_{5/2})^{-1} \otimes \nu g_{9/2}^{-1} \rightarrow \pi g_{9/2}^2(p_{3/2}/f_{5/2})^{-1} \otimes \nu g_{9/2}^{-3}$ for the negative-parity band in ^{86}Y. Figure 4 shows that the calculated values for these states between $I = 14\hbar$ and $I = 17\hbar$ are missing. This is caused by the fact that the level crossing connected with a sharp backbending phenomenon [20] is not described well in the cranking approximation, and converged solutions for these angular-momentum values could not be obtained at present.

In order to examine the shears mechanism for the magnetic rotational bands in the nuclei ^{86}Y, we show in Figs. 5(a) and 5(b) the proton and the neutron angular-momentum vectors J_π and J_ν as well as the total angular-momentum vectors $J_{\rm tot} = J_\pi + J_\nu$ at both the minimum and the maximum rotational frequencies in TAC-RMF calculations for the negative-parity band before and after the backbend of ^{86}Y. The proton and neutron angular momenta J_π and J_ν are defined as

$$J_\pi = \langle \hat{J}_\pi \rangle = \sum_{p=1}^{Z} \langle p \mid \hat{J} \mid p \rangle, \tag{2}$$

$$J_\nu = \langle \hat{J}_\nu \rangle = \sum_{n=1}^{N} \langle n \mid \hat{J} \mid n \rangle. \tag{3}$$

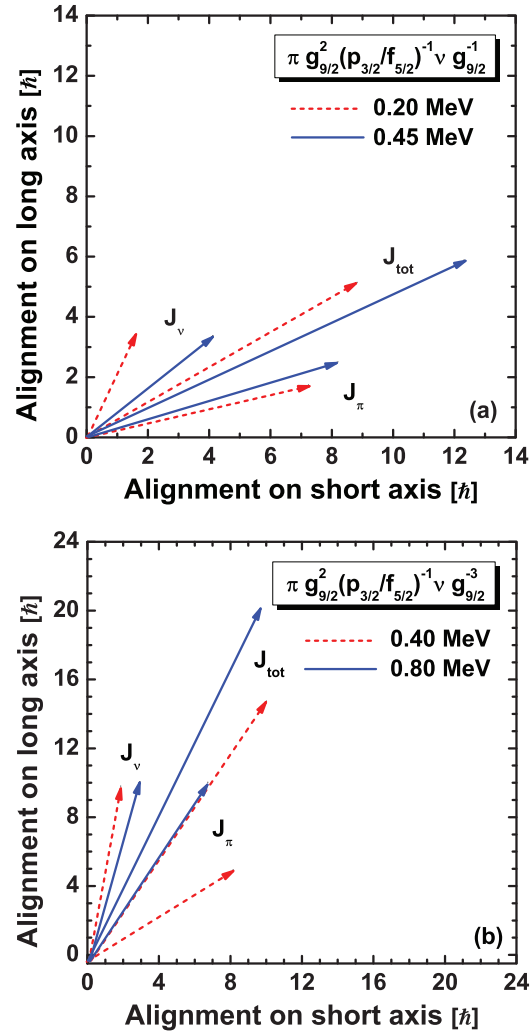

FIG. 5. (Color online) Composition of the total angular momentum at both the minimum and the maximum rotational frequencies in the TAC-RMF calculations for the negative-parity band. Upper (a) and lower (b) panels represent the results before and after the backbend, respectively.

where the sum runs over all the proton (or neutron) levels occupied in the cranking wave function in the intrinsic system.

For the magnetic dipole band in ^{86}Y, the contributions to the angular momenta come mainly from the high-j orbitals $g_{9/2}$ for both neutron(s) and protons. At the bandhead, the proton particle(s) filling the bottom of the $g_{9/2}$ shell mainly contribute to the proton angular momentum along the short axis, and the neutron hole at the upper end of the $g_{9/2}$ shell mainly contributes to the neutron angular momentum along the long axis. In this case, the proton and neutron angular-momentum vectors form the two blades of the shears. As the frequency increases, the two blades move toward each other to provide larger angular momentum, while the direction of the total angular momentum does not change much. In this way, the shears mechanism is clearly presented. By comparing the upper panel (before backbend) with the lower one (after backbend) in Fig. 5, one finds that after the backbend the neutron angular-momentum vectors are considerably larger,

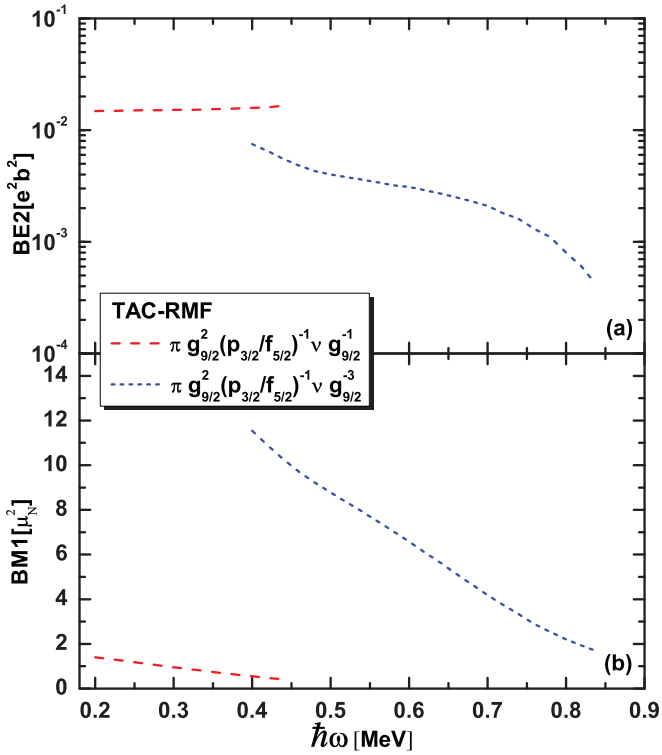

FIG. 6. (Color online) Reduced $E2$ transition probabilities $B(E2)$ (a) and reduced $M1$ transition probabilities $B(M1)$ (b) as functions of the total angular momentum in the TAC-RMF calculations.

because they contain the contributions of an aligned pair of $g_{9/2}$ neutron holes.

A typical characteristic of magnetic rotation is strongly enhanced $M1$ transitions at low spins as well their decreasing tendency with increasing angular momentum. In contrast to the enhanced $M1$ transitions, the $E2$ transitions are very weak for magnetic rotational bands. In Figs. 6(a) and 6(b) we show the calculated $B(E2)$ as well as $B(M1)$ values as functions of the total angular momentum for the negative-parity band in ^{86}Y. For the $B(M1)$ values, the smooth decreasing tendency shown in the negative-parity band before and after the backbend obviously presents further evidence of the shears mechanism. It should be pointed out that, although there are no experimental $B(M1)$ values at present, the calculated $B(M1)$ values ($0.4 \sim 1.4\mu_N^2$) are in the same order as the experimental $B(M1)$ values ($0.2 \sim 0.8\mu_N^2$) of a similar band in neighboring nucleus ^{84}Rb [17]. In addition, owing to the gain of angular momentum from the alignment of a pair of $g_{9/2}$ neutrons after the backbend and the very similar shears angles for the negative-parity band before and after the backbend, the $B(M1)$ values after the backbend are much larger than the corresponding values before the backbend.

The calculated $B(E2)$ values are shown in the upper panel of Fig. 6 as functions of the total angular momentum. In contrast to the large $B(M1)$ values (about several μ_N^2), the $B(E2)$ values are very small for both bands [<0.05 $(e\text{b})^2$]. This will lead to large calculated $B(M1)/B(E2)$ values [$>25\mu_N^2$ $(e\text{b})^{-2}$], and indicates that the rotation has prominent magnetic character. Unfortunately, lifetimes have not been extracted in Ref. [18]. However, the fact that there are strong $M1$ transitions but no crossover $E2$ transitions shows that the experimental $B(M1)/B(E2)$ must be very large in the negative-parity band. At relatively lower spins of the negative band, the $B(E2)$ values show a roughly constant trend. It implies that the nucleus stays at a small deformation along the band. Moreover, with increasing spin, a sharp decreasing trend of the $B(E2)$ values can be found from the calculated results for the band after the backbend. This indicates a signal for the termination of the corresponding shears band.

IV. SUMMARY

In conclusion, the positive-parity yrast band and the negative-parity $M1$ band observed in the odd-odd nucleus ^{86}Y have been studied. It is found that the positive-parity yrast band shows a signature splitting and signature inversion, and the inversion point occurs around spin $13\hbar$, somewhat shifted to higher spin when compared with the neighboring isotope ^{84}Y and the isotone ^{84}Rb. It is likely that this shift has its origin in the competition between single-particle and collective degrees of freedom. In addition, the relatively constant values of kinematic moments of inertia in a rather large range of spins values suggest a collective rotational interpretation for the high spin states of the yrast band.

The regular negative-parity $M1$ band displays characteristics of magnetic rotation and a backbend occurs at $I^\pi \sim 16^{(-)}\hbar$ due to the alignment of a $g_{9/2}$ neutron-hole pair. The configuration $\pi g_{9/2}^2(p_{3/2}/f_{5/2})^{-1} \otimes \nu g_{9/2}^{-1}$ before the alignment and the configuration $\pi g_{9/2}^2(p_{3/2}/f_{5/2})^{-1} \otimes \nu g_{9/2}^{-3}$ after the alignment have been assigned. The fully microscopic and self-consistent TAC-RMF model based on the point-coupling density functional PC-PK1 has been applied to examine the shears mechanism in the negative-parity band. The angular momenta, titled angles, and reduced $M1$ and $E2$ transition probabilities have been calculated. The experimental angular momenta as a function of rotational frequency have been studied and compared with the TAC-RMF calculations, and good agreement has been obtained, showing that the TAC-RMF calculations can reproduce the moments of inertia rather well. The calculated decrease of $B(M1)$ values with increasing angular velocity indicates the appearance of a shear mechanism in ^{86}Y. In addition, a shear mechanism has been clearly illustrated in the candidate band for MR. However, more investigations in the future, such as lifetime measurements, should be useful to make a conclusive interpretation. Additional work is necessary for systematic calculations for other isotopes in this region.

ACKNOWLEDGMENTS

The authors thank J. Meng, S. Q. Zhang, and P. W. Zhao for useful discussions. We are grateful to P. Ring for his critical reading on the manuscript. This work is partially supported by the NSFC (Grants No. 11075214, No. 11175259, No. 11205068, and No. 11205069) and CPSC (Grant No. 2012M520667).

[1] R. Schubart *et al.*, Nucl. Phys. A **591**, 515 (1995).
[2] G. B. Han *et al.*, Chin. Phys. Lett **16**, 487 (1999).
[3] D. Bucurescu *et al.*, Nucl. Phys. A **705**, 3 (2002).
[4] S. D. Paul, H. C. Jain, S. Chattopadhyay, M. L. Jhingan, and J. A. Sheikh, Phys. Rev. C **51**, 2959 (1995).
[5] S. Chattopadhyay, H. C. Jain, S. D. Paul, J. A. Sheikh, and M. L. Jhingan, Phys. Rev. C **49**, 116 (1994).
[6] S. Frauendorf, J. Meng, and J. Reif, in Proceedings of the Conference on Physics from Large γ-ray Detector Arrays, Lawrence Berkeley National Laboratory Report No. LBL-35687, 1994 (unpublished).
[7] S. Frauendorf, Rev. Mod. Phys **73**, 463 (2001).
[8] C. Y. He *et al.*, Phys. Rev. C **81**, 057301 (2010).
[9] C. Y. He *et al.*, Phys. Rev. C **83**, 024309 (2011).
[10] C. B. Li *et al.*, Nucl. Phys. A **892**, 34 (2012).
[11] R. Ma *et al.*, Phys. Rev. C **41**, 2624 (1990).
[12] E. S. Paul *et al.*, Phys. Rev. C **41**, 1576 (1990).
[13] R. M. Clark *et al.*, Nucl. Phys. A **562**, 121 (1993).
[14] G. Baldsiefen *et al.*, Nucl. Phys. A **574**, 521 (1994).
[15] H. Schnare *et al.*, Phys. Rev. Lett **82**, 4408 (1999).
[16] J. Döring, D. Ulrich, G. D. Johns, M. A. Riley, and S. L. Tabor, Phys. Rev. C **59**, 71 (1999).
[17] R. Schwengner *et al.*, Phys. Rev. C **66**, 024310 (2002).
[18] C. Rusu *et al.*, Nucl. Phys. A **818**, 1 (2009).
[19] S. Frauendorf, Nucl. Phys. A **557**, 259 (1993).
[20] J. Peng, J. Meng, P. Ring, and S. Q. Zhang, Phys. Rev. C **78**, 024313 (2008).
[21] P. W. Zhao *et al.*, Phys. Lett. B **699**, 181 (2011).
[22] J. Meng, J. Peng, S. Q. Zhang, and P. W. Zhao, Front. Phys. **8**, 55 (2013).
[23] D. Bucurescu *et al.*, J. Phys. G **10**, 1189 (1984).
[24] A. J. Kreiner and M. A. J. Mariscotti, Phys. Rev. Lett **43**, 1150 (1979).
[25] P. C. Womble *et al.*, Phys. Rev. C **47**, 2546 (1993).
[26] G. García-Bermúdez, H. Somacal, M. A. Cardona, A. Filevich, E. Achterberg, and L. Szybisz, Phys. Rev. C **51**, 1181 (1995).
[27] A. Bohr and B. R. Mottelson, Phys. Scr. **24**, 71 (1981).
[28] R. Bengtsson, S. Frauendorf, and F. R. May, At. Data Nucl. Data Tables **35**, 15 (1986).
[29] J. Li, S. Q. Zhang, and J. Meng, Phys. Rev. C **83**, 037301 (2011).
[30] J. Peng, J. Meng, and S. Q. Zhang, Phys. Rev. C **68**, 044324 (2003).
[31] J. W. Tepel, Nucl. Data Sheets **25**, 553 (1978).
[32] S. Frauendorf and J. Meng, Z Phys. A **356**, 263 (1996).
[33] Y. K. Gambhir, P. Ring, and A. Thimet, Ann. Phys. (NY) **198**, 132 (1990).
[34] P. Ring, Prog. Part. Nucl. Phys. **37**, 193 (1996).
[35] J. Meng *et al.*, Prog. Part. Nucl. Phys. **57**, 470 (2006).
[36] H. Madokoro, J. Meng, M. Matsuzaki, and S. Yamaji, Phys. Rev. C **62**, 061301(R) (2000).
[37] D. Steppenbeck *et al.*, Phys. Rev. C **85**, 044316 (2012).
[38] K. Y. Ma *et al.*, Eur. Phys. J. A **48**, 82 (2012).
[39] L. F. Yu, P. W. Zhao, S. Q. Zhang, P. Ring, and J. Meng, Phys. Rev. C **85**, 024318 (2012).
[40] P. W. Zhao, Z. P. Li, J. M. Yao, and J. Meng, Phys. Rev. C **82**, 054319 (2010).
[41] P. W. Zhao, J. Peng, H. Z. Liang, P. Ring, and J. Meng, Phys. Rev. Lett. **107**, 122501 (2011).
[42] P. W. Zhao, J. Peng, H. Z. Liang, P. Ring, and J. Meng, Phys. Rev. C. **85**, 054310 (2012).
[43] X. W. Li *et al.*, Phys. Rev. C **86**, 057305 (2012).
[44] W. Koepf and P. Ring, Nucl. Phys. A **493**, 61 (1989).